Thermochimica Acta 694 (2020) 178796

Contents lists available at ScienceDirect

Thermochimica Acta

journal homepage: www.elsevier.com/locate/tca

Study the hematite reduction kinetics by the magnetic method

P.A. Chernavskii *, G.V. Pankina, S.V. Maksimov, N.V. Kim, A.A. Novakova

Department of Chemistry Lomonosov Moscow State University 1-3 Leninsky Gory, Moscow 119991 Russia

ARTICLE INFO

Keywords:
Reduction
Iron oxides
Hydrogen
Particle sizes
Magnetic properties

ABSTRACT

This study is devoted to the reduction of Fe_2O_3 supported on silica gel in H_2 in the temperature range of 290–600 °C. A continuous magnetization measurement method was used to obtain the temperature programmed reduction (TPR) profile. The influence of the external magnetic field on the dynamics of the process is investigated. It was shown that the TPR profile depends both on the magnitude of the applied field and on the particle size of hematite.

1. Introduction

The reduction of Fe_2O_3 with hydrogen was a subject of numerous studies [1–7], but there still have been differing opinions concerning the reaction route, even for unsupported samples.

Thus, there are TPR studies, which point to the two-step mechanism, i.e. $Fe_2O_3 \rightarrow Fe_3O_4 \rightarrow Fe$ [1–4], and there are reports indicating the three-step mechanism, i.e. $Fe_2O_3 \rightarrow Fe_3O_4 \rightarrow FeO \rightarrow Fe$ [1–7]. Kock [2] et al. emphasize that stabilization of an FeO phase during reduction is indicative of a considerable metal(oxide)-support interaction. Moreover, the formation of the phase is observed at a temperature below the boundary of the thermodynamic stability of wüstite. The studies [8–10] also showed the stability of the phase at temperatures below 570 °C. The stabilization of the FeO phase upon reduction occurs due to the interaction of the oxide with the support.

The aim of this examination is to clarify mechanism of Fe_2O_3 reduction. This knowledge is of great importance when TPR method is applied to characterization of iron supported catalysts. TPR method is a relatively simple technique, but analysis of the experimental results is often difficult. The problem of H_2 depletion in the course of TPR tests has been revealed and extensively discussed by Monti and Baiker [11]. As a result, they proposed that the experimental parameter of TPR test should be selected so as to get only a small decline of H_2 concentration.

Water is the inevitable product in TPR experiment and its concentration generally changes in the course of TPR test from a negligibly small value to a significant value, i.e. a few orders of magnitude, and may radically change position and shape of the recorded TPR profile.

The traditional TPR method involves the use of a hydrogen – argon mixture in which the hydrogen concentration does not exceed 10 % as a reducing agent. Using the method of continuous in situ magnetization measurement [12–15], pure hydrogen can be used, and the change in the magnetization during the reaction can be recorded as a response. The high sensitivity of the method allows one to obtain TPR profiles with relatively small masses of the test substance 10−20 mg. At a hydrogen flow rate of about 30 mL / min and an analyte volume of 0.04 cm^3, the space velocity is $\approx 45 \cdot 10^3$ 1 / h, which makes it possible to exclude the influence of diffusion processes on the shape of TPR profiles.

2. Material and experimental procedure

2.1. Materials

The following substances were used as test substances: hematite (Fe_2O_3 - Sigma-Aldrich) powder < 5 μm, > 96 % and iron on silica gel. Iron nitrate was used as a precursor ($Fe(NO_3)_3 \cdot 9H_2O$) Iron(III) nitrate nonahydrate Sigma-Aldrich. CARIACT silica gel grade Q-30 (30 nm the average pore size in silica gel) manufactured by Fuji Silysia Chemical, Ltd was used as a support. Here the number means the average pore size in silica gel. The preassigned content of iron was of 5, 10 and 15 mass%. These samples are denoted as for example 5/Q where the first digit reflects the iron content.

Catalysts were prepared by incipient wetness impregnation of the support with aqueous solutions of hydrous iron nitrate. After the impregnation, the catalysts were dried overnight in an oven at 100 °C. Then they were calcined in air at 400 °C for 6 h with 1 °C/min temperature ramping.

---

* Corresponding author at: Department of Chemistry Lomonosov Moscow State University 1-3 Leninsky Gory, Moscow 119991 Russia; Institute of Organic Chemistry N.D. Zelinsky, Russian Academy of Sciences, Leninsky Prospekt, 47 119991, Moscow, Russia.

E-mail address: chern5@inbox.ru (P.A. Chernavskii).

https://doi.org/10.1016/j.tca.2020.178796
Received 13 April 2020; Received in revised form 16 September 2020; Accepted 5 October 2020

Below is a block diagram of the Fe / SiO2 synthesis process:

Solution $Fe(NO_3)_3{\cdot}9H_2O + SiO_2 \rightarrow$(dried overnight in an oven at 100 °C)→(calcined in air at 400 °C for 6 h)

2.2. Temperature-programmed reduction

Magnetic studies of the samples were carried out on a vibration magnetometer in situ regime. The test sample (10 mg) was placed in a measuring cell of the vibrating magnetometer, [15] which is a flow-through microreactor with the internal volume of 0.3 cm^3. The test sample was

clamped between two membranes of porous quartz. In a non-isothermal experiment, the sample was heated to a predetermined temperature in H_2 with a flow rate of 30 mL min^{-1}. The heating rate ranged from 0.1 °C/s to 0.8 °C/s to a predetermined temperature, while a change in magnetization was recorded continuously at a frequency of 1 Hz. The low inertia micro-furnace allows rapid cooling of the test sample and interrupts the reduction process at a given temperature.

2.3. X-Ray diffraction

Diffraction patterns were recorded on a PANalytical Empyrean diffractometer in Bragg-Brentano geometry (ϑ mode - 2ϑ scans, 40 mA, 40 kV) in increments of 0.026 degrees, in the range of angles from 5 to 100 degrees using a Pixel3D detector. The anode material is Cu. Diffraction patterns were analyzed using HighScore Plus PANalytical software with full-profile analysis. After cooling in hydrogen, the samples were passivated in a stream of technical Ar, and then transferred to a diffractometer.

2.4. Transmission electron microscopy

Transmission electron microscopy (TEM) analyses were carried out on a JEOL JEM-2100 F microscope at a resolution of 0.1–0.2 nm and accelerating voltage of 200 kV. Prior to the analysis, the sample was thoroughly ground in an agate mortar in ethanol and left for few hours. Then a drop of supernatant liquid was deposited onto a polymer film located on a copper grid. The particle size distribution was obtained by visual analysis of micrographs using "Image-Pro Plus 6.0″ software. To build a histogram, 600–1000 particles were taken into account.

3. Results

Fig. 1 (a and b) shows the TPR profiles of the samples 15/Q, 10/Q and 5/Q obtained in a magnetic field of 60 Oe (a) and in a field of 5 kOe (b).

The increase in magnetization in the temperature range from 250 to 350 °C is due to the reduction of Fe_2O_3 to magnetite (ferrimagnet). The subsequent decrease in magnetization, in our opinion, is caused by the formation of antiferromagnetic wüstite (Fig. 1 a). The subsequent increase in magnetization is due to the reduction of wüstite to metallic iron. The results of X-ray diffraction of samples obtained by cooling from points A, B, and C (Fig. 1. a) are shown in Fig. 2.

The results of the X-ray phase study show that the increase in magnetization at point A (Fig. 1a) corresponds to the formation of magnetite. The decrease in magnetization at point C is due to the formation of wüstite (Fig. 1b), and the subsequent increase in magnetization is caused by the formation of iron. In this way, X-ray diffraction data confirm the above interpretation of the change in magnetization during the TPR.

Fig. 3 shows the TPR profiles for 5/Q at field strengths of 60 Oe and 5 kOe. It is characteristic that an increase in the magnetic field strength does not qualitatively affect the TPR profile of the sample 5/Q.

The TPR profiles obtained in a field of 5 kOe demonstrate significant differences in the temperature range above 350 °C (Fig. 1. b). In this case, a sharp decrease in the magnetization is not observed for the samples 10/Q and 15/Q. Fig. 4 shows the temperature dependences of magnetization for various values of applied magnetic field in the process redaction of 15/Q.

It can be seen that an increase in the magnetic field strength leads to a sequential change in the nature of the TPR profiles. In Fig. 5 (a) and (b) show the TPR profile and XRD spectra for 15/Q at points A, B, and C at 5 kOe.

Judging by the data of the XRD, magnetite is present at points A, B and C, but at the point C, there is also the presence of wüstite. Upon reaching a temperature of 440 °C, the process magnetite reduction to iron begins to prevail.

An analysis of the TEM image shows that the average particle sizes of hematite in samples 5/Q, 10/Q, 15/Q are 3, 9, and 13 nm, respectively. The particle size distribution is well described by the lognormal distribution. In Figs. 6, 7 and 8 show microphotographs and size distributions for 5/Q, 10/Q and 15/Q. The average particle size grows linearly with an increase in the concentration of iron supported on the silica gel.

TEM images show that the TPR profile substantially depends on the particle size of hematite. Moreover, for particles of 3 nm, the TPR profile is qualitatively independent of the magnitude of the applied field. With an increase in particle size to 9 nm, a qualitative change in the shape of the TPR profile is observed (Fig. 1b).

4. Discussion

To explain the above results, the following circumstances must be taken into account. The observed change in the magnetization with increasing temperature is due to at least two factors. Firstly, this is a change in the magnetization with increasing temperature. Secondly, this is a change in the magnetization associated with chemical reactions. An increase in magnetization with increasing temperature indicates a chemical reaction. In the case considered above, this is the reduction of oxide (Fe_2O_3) located in the pores of silica gel. A decrease in magnetization can be caused both by the transition of a ferromagnetic to a nonmagnetic state due to a chemical reaction and by the dependence of magnetization on temperature. The results of the XRD indicate the

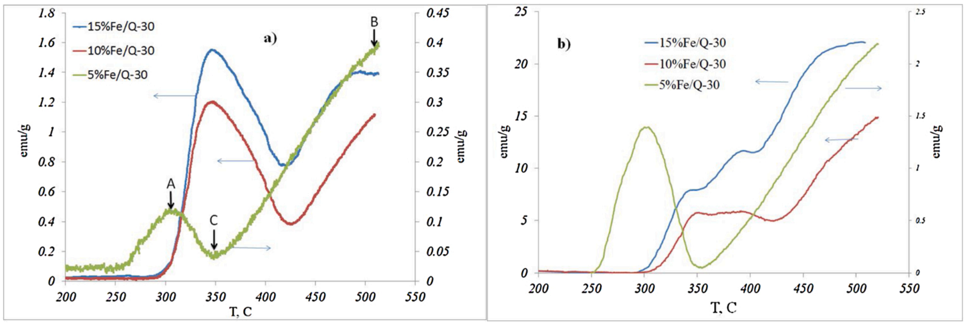

Fig. 1. TPR profiles of the samples 15/Q-30, 10/Q and 5/Q obtained in a magnetic field of Oe (a) and in a field of 5 kOe (b).

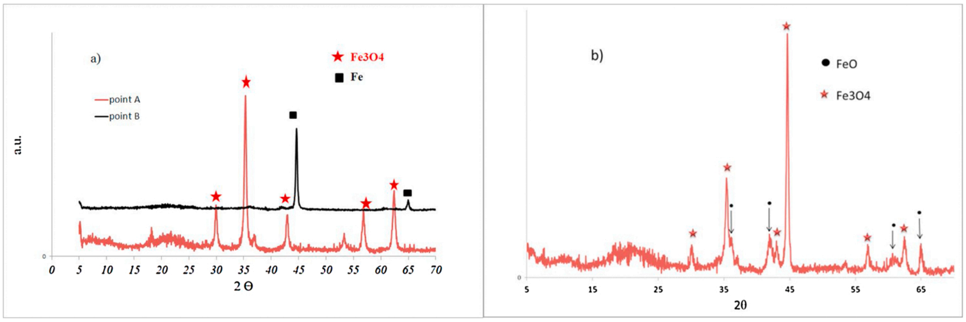

Fig. 2. X-ray diffraction patterns of samples 5/Q obtained at points A, B (a) and C (b).

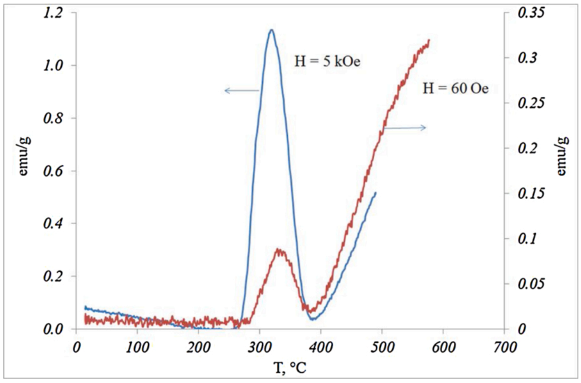

Fig. 3. TPR profile 5/Q at field strengths 60 Oe and 5 kOe.

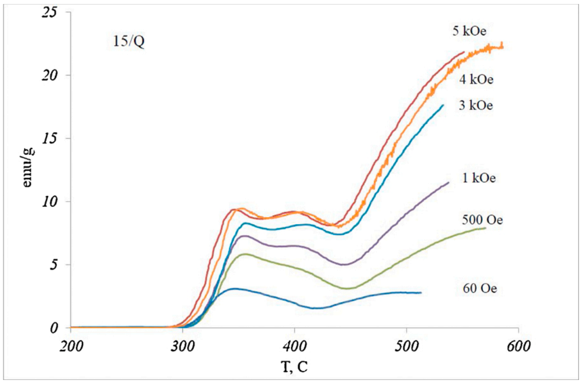

Fig. 4. TPR profiles the samples 15/Q at various values of the external magnetic field.

chemical nature (formation of wüstite) of the decrease in magnetization in the case of reduction in a low magnetic field (Fig. 1a).

It should be noted that the sequence of reduction reactions substantially depends not only on the magnitude of the applied magnetic field, but also on the size of the oxide particles. The TEM results show that for relatively small oxide particle sizes (average size 3 nm), the applied field does not affect the quality of the process (Fig. 3). In this case, both in the 60 Oe field and in the 5 kOe field, the hematite is gradually reduced to iron in accordance with the following equation:

$$3Fe_2O_3 + H_2 = 2Fe_3O_4 + H_2O \tag{1}$$

$$2Fe_3O_4 + 2H_2 = 6FeO + 2H_2O \tag{2}$$

$$6FeO + 6H_2 = 6Fe + 6H_2O \tag{3}$$

With an increase in the average particle size to 9–13 nm, a change in the magnetization with increasing temperature in a magnetic field of more than 500 Oe undergoes qualitative changes (Fig. 4). A more complex picture is observed when reduction in a relatively strong magnetic field (Fig. 5). The sequence of transformations accompanying a change in magnetization includes all the reactions of reduction and disproportionation:

$$Fe_3O_4 + H_2 = 3FeO + H_2O \tag{4}$$

$$FeO + H_2 = Fe + H_2O \tag{5}$$

$$4FeO = Fe_3O_4 + Fe \tag{6}$$

We have previously shown that the reduction of magnetite to iron in a magnetic field of 5 kOe proceeds bypassing the stage of wüstite formation, while wüstite is formed in a relatively weak field of 60 Oe [16]. The influence of an external magnetic field on topochemical reactions currently has no strict physically justified explanation. Since the recovery process involves the formation of nucleation centers [17,18], it can be assumed that an external magnetic field affects the spin state of surface centers.

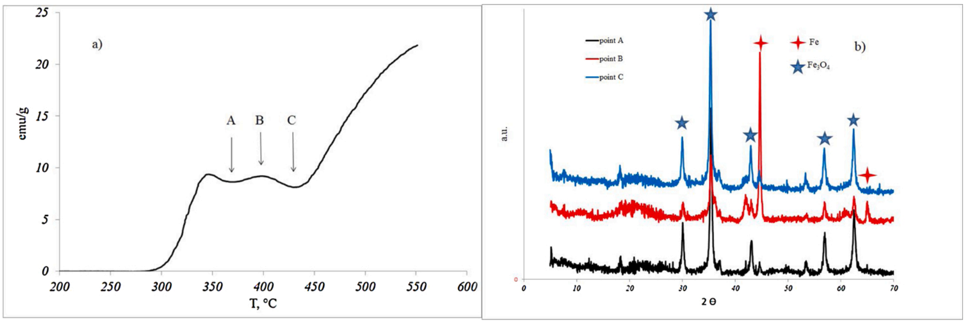

Fig. 5. a) TPR profiles the samples 15/Q and b) XRD for points A, B and C at 5 kOe.

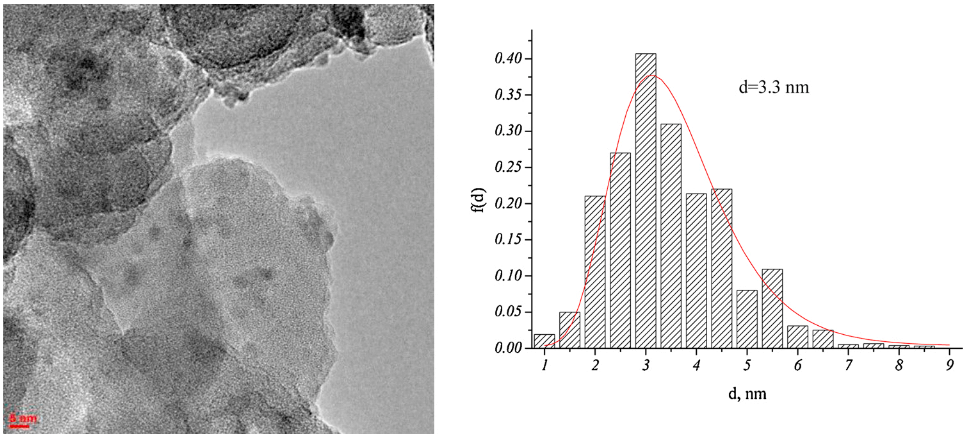

Fig. 6. TEM image and particle size distribution for 5/Q.

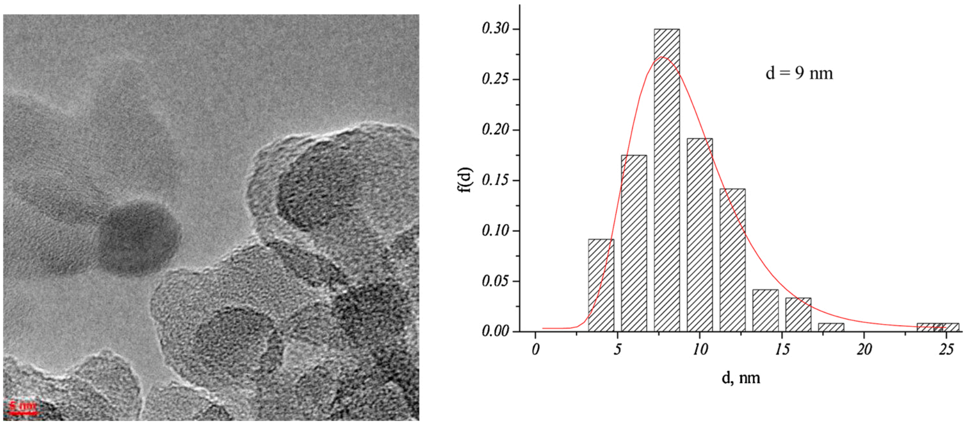

Fig. 7. TEM image and particle size distribution for 10/Q.

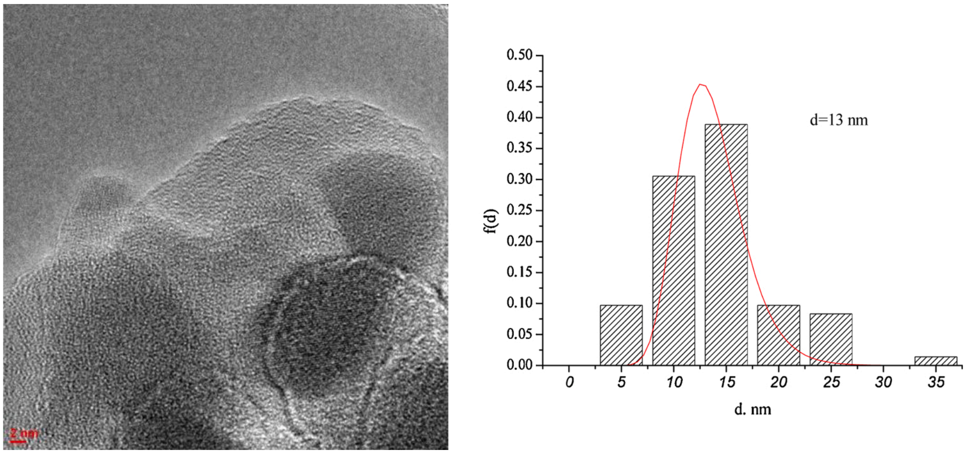

Fig. 8. TEM image and particle size distribution for 15/Q.

5. Conclusion

The use of the continuous measurement of magnetization method to study topochemical processes made it possible to detect the influence of an external magnetic field on the qualitative and quantitative features of the TPR profiles. It turned out that the effect of the magnetic field depends on the size of the magnet particles. The TPR profile for hematite particles with an average size of 3 nm does not qualitatively depend on the magnitude of the applied magnetic field. However, an increase in the average size to 9 nm leads to both quantitative and qualitative changes in the TPR profile. In relatively small fields, the hematite reduction proceeds through the formation of wüstite. However, with an increase in the magnetic field, a decrease in the role of the formation stage of wüstite is observed. In the field of 3 kOe and more, the recovery proceeds almost bypassing the stage of formation of wüstite. At present, we cannot provide a sufficiently reasonable explanation for the observed effects. We hope that further studies of the magnetic field influence on topochemical processes will shed light on the mechanism the magnetic field action.

AuthorsStatement

Chernavskii P.A.
The experiment idea, magnetic measurements, data and the main text of the manuscript preparation.
Pankina G.V.
The sample synthesis and figures preparation.
Maksimov S.V.
The electronic microscopy measurements and interpretation
Kim N.V.
X-Ray measurements
Novakova A.A.
X-Ray measurements results interpretation

Declaration of Competing Interest

The authors declare that they have no known competing financial interests or personal relationships that could have appeared to influence the work reported in this paper.

Acknowledgments

This research did not receive any specific grant from funding agencies in the public, commercial, or not-for-profit sectors.

References

[1] A. Pineau, N. Kanari, I. Gaballah, Kinetics of reduction of iron oxides by H2 Part II. Low temperature reduction of magnetite, Thermochim. Acta 456 (2007) 75–88, https://doi.org/10.1016/j.tca.2007.01.014.

[2] J.H.M. Kock, H.M. Fortuin, J.W. Geus, The reduction behavior of supported iron catalysts in hydrogen or carbon monoxide atmospheres, J. Catal. 96 (1985) 261–275, doi.org/10.1016/00219517(85)90379-3.

[3] G.J. Wimmers, P. Arnoldy, J.A. Moulijn, Determination of the reduction mechanism by temperature-programmed reduction: application to small iron oxide (Fe2O3) particles, J. Phys. Chem. 90 (1986) 1331–1337, https://doi.org/10.1021/j100398a025.

[4] G. Munteanu, L. Ilieva, D. Andreeva, Kinetic parameters obtained from TPR data for α-Fe_2O_3 and Auα-Fe2O3 systems, Termochim. Acta 291 (1997) 171–177, doi.org/10.1016/S00406031(96)03097-3.

[5] H.Y. Lin, Y.W. Chen, Ch.P. Li, The mechanism of reduction of iron oxide by hydrogen, Termochim. Acta 400 (2003) 61–67, doi.org/10.1016/S0040-6031(02)00478-1.

[6] Daniel Spreitzer, Johannes Schenk, Reduction of Iron oxides with hydrogen—a review, steel research int. 90 (2019) 1900108, https://doi.org/10.1002/srin.201900108.

[7] W.K.J.y ŕzwiak, E. Kaczmarek, T.P. Maniecki, W. Ignaczak, W. Maniukiewicz, Reduction behavior of iron oxides in hydrogen and carbon monoxide atmospheres, Appl.Catal. A: Gen. 326 (2007) 17–27, doi.org/10.1016/j.apcata.2007.03.021.

[8] Cheng-Hua Zhang, Hai-Jun Wan, Yong Yang, Hong-Wei Xiang, Yong-Wang Li, Study on the iron–silica interaction of a co-precipitated Fe/SiO2 Fischer–Tropsch synthesis catalyst, Catal. Commun. 7 (2006) 733–738, https://doi.org/10.1016/j.catcom.2006.03.018.

[9] P.A. Chernavskii, V.V. Kiselev, L.I. Baranova, A.P. Kuprin, A.N. Grechenko, V. V. Lunin, Characteristics of hydrogen reduction of iron-oxides applied on silica-gel, Russ. J. Phys. Chem. 65 (1991), 1675.

[10] A. Chernavskii, V.V. Kiselev, V.V. Lunin, Mechanism of reduction of iron oxides deposited on silica gel, Russ. J. Phys. Chem. 66 (1992), 2712.

[11] D.A.M. Monti, A. Baiker, Temperature-programmed reduction. Parametric sensitivity and estimation of kinetic parameters, J. Catal. 83 (1983) 323–335, doi.org/10.1016/00219517(83)90058-1.

[12] P.A. Chernavskii, A.Y. Khodakov, G.V. Pankina, J.-S. Girardon, E. Quinet, In situ characterization of the genesis of cobalt metal particles in silica-supported Fischer-Tropsch catalysts using Foner magnetic method, Appl. Catal. A Gen. 306 (2006) 108–119, doi.org/10.1016/j.apcata.2006.03.033.

[13] P.A. Chernavskii, G.V. Pankina, V.V. Lunin, Magnetometric methods of investigation of supported catalysts, Russ. Chem. Rev. 80 (6) (2011) 579–604, doi.org/10.1070/RC2011v080n06ABEH004187.

[14] P.A. Chernavskii, G.V. Pankina, A.S. Lermontov, Kinetics of reduction of Co oxide nanoparticles on silica gel, Russ. J. Phys. Chem. 79 (2005) 875–880.

[15] P.A. Chernavskii, B.S. Lunin, R.A. Zakharyan, G.V. Pankina, N.S. Perov, Experimental setup for investigating topochemical transformations of ferromagnetic nanoparticles, Instrum. Exp. Tech. 57 (2014) 78–81, dx.doi.org/10.7868/S0032816214010030.

[16] P.A. Chernavskii, M.I. Ivantsov, V.V. Lunin, Influence of an external magnetic field on the dynamics of magnetite reduction by hydrogen, Russian Chemical Bulletin, International Edition 68 (2019) 1946–1948.

[17] Mohamed Elzohiery, Hong Yong Sohn, Yousef Mohassab, Kinetics of hydrogen reduction of magnetite concentrate particles in solid state relevant to flash ironmaking, Steel research int. 87 (2016), https://doi.org/10.1002/srin.201600133, 9999.

[18] K. Piotrowski a, K. Mondalb, T. Wiltowski b,c, P. Dydod, G. Rizeg, Topochemical approach of kinetics of the reduction of hematite to wüstite, Chem. Eng. J. 131 (2007) 73–82, https://doi.org/10.1016/j.cej.2006.12.024.